Rock and Soil Mechanics

Volume 42 | Issue 11 Article 5

2-23-2022

Mechanical properties and strength criterion of Zhanjiang structured clay in three-dimensional stress state

Bing-heng LIU
University of Chinese Academy of Sciences, Beijing 100049, China

Ling-wei KONG
University of Chinese Academy of Sciences, Beijing 100049, China, lwkong@whrsm.ac.cn

Rong-jun SHU
University of Chinese Academy of Sciences, Beijing 100049, China

Tian-guo LI
University of Chinese Academy of Sciences, Beijing 100049, China

Custom Citation

LIU Bing-heng, KONG Ling-wei, SHU Rong-jun, LI Tian-guo, . Mechanical properties and strength criterion of Zhanjiang structured clay in three-dimensional stress state[J]. Rock and Soil Mechanics, 2021, 42(11): 3090-3100.

Rock and Soil Mechanics 2021 42(11): 3090−3100 ISSN 1000−7598
https: //doi.org/10.16285/j.rsm.2021.5396 rocksoilmech.researchcommons.org/journal

Mechanical properties and strength criterion of Zhanjiang structured clay in three-dimensional stress state

LIU Bing-heng[1, 2], KONG Ling-wei[1, 2], SHU Rong-jun[1, 2], LI Tian-guo[1, 2]

1. Institute of Rock and Soil Mechanics, Chinese Academy of Sciences, Wuhan, Hubei 430071, China;
2. University of Chinese Academy of Sciences, Beijing 100049, China

Abstract: In order to investigate the mechanical properties of Zhanjiang structured clay in the three-dimensional stress state and the influence of structure on its strength criterion, a series of undrained true triaxial tests of different intermediate principal stress ratios, *b*-values, with equal mean principal stress, *p*-values, and undrained plane strain tests was carried out. The results are as follows. When *p* is less than or greater than the yield stress of the structure, the q-ε_1 curves are strain softening and mild strain hardening type in general. The q-ε_1 curves of true triaxial tests with different *b*-values are similar in shape. As *b*-value increases, the large principal strain corresponding to the *q* peak point shows the decreasing trend. Under different *b*-values, the effective cohesion decreases with increasing *b*-values, while the effective friction angle increases with increasing *b*-values. The effective cohesion and friction angle for the plane strain compression tests are between the effective cohesion and friction angle corresponding to b=0.25 and b=0.50. Influenced by the structure of clay, the strength criterion on π plane is applicable to the Lade-Duncan criterion when *p*-values are less than the yield stress of structure, while it is more applicable to the generalized nonlinear strength theory based on Mises criterion and Lade-Duncan criterion when *p*-values are greater than the yield stress of structure. For plane strain tests, the *b*-values of Zhanjiang clay under plane strain loading and unloading conditions are between 0.18 and 0.29 at failure, and the strength at failure can be approximated by the generalized plane strain strength criterion based on the general Mises and Lade-Duncan plane strain strength criterion.

Keywords: Zhanjiang clay; strength criterion; structure; true triaxial test; anisotropy

1 Introduction

With the rapid development of the economy in southeastern coastal areas of China, a growing number of traffic engineering and construction engineering are put on the agenda. Soft clay, as a widely involved object in engineering projects, is characterized by high water content, high compressibility and low permeability, and foundation failure often occurs during the construction process. Therefore, the mechanical properties of soft soils, especially the strength criterion, are essential for engineering safety. The soil in slopes or around foundation pits and tunnels is often under three-dimensional stress state[1], it is affected by three independent principal stresses, that is, the major principal stress σ_1, the intermediate principal stress σ_2 and the minor principal stress σ_3. In engineering practice, most of the engineering design is based on the test results of the traditional triaxial path, that is, the axisymmetric stress path. However, there are significant differences in boundary conditions and stress states between the conventional triaxial test and the true triaxial test[2−3]. There is a certain error in selecting the results of traditional triaxial tests as the basis for engineering design[4]. Many scholars have investigated the strength of soft soil under true triaxial stress states to overcome the above problems[5−8], and many strength criteria considering the intermediate principal stress have been established. For example, Lade[9] presented the Lade-Duncan strength criterion according to the true triaxial tests; Matsuoka et al.[10] proposed the SMP strength criterion based on the concept of spatial sliding surface; Yu[11] established the double shear stress strength theory, etc.

In fact, natural soft clay often has certain structural properties. The structured clay is widely distributed in some southeastern coastal areas of China, such as Shanghai clay and Hangzhou muddy clay. The mechanical properties of these clays are affected by the structural properties[12]. In order to further explore the influence of structural properties on soil deformation and strength, some scholars have studied the soils with structural properties through the field test[13], consolidation test[14] and triaxial test[15]. The stress states of soils in the above studies are mainly axisymmetric, while there are fewer studies to investigate the influence of structural properties on the mechanical properties of soils under three-dimensional stress; in addition, when studying the soil strength criterion under three-dimensional stress, the effect of soil structural properties is less considered, so it is necessary to further investigate the soil mechanical properties and strength criterion under three-dimensional stress state by considering the influence of structural properties.

In this paper, Zhanjiang structural clay, which is known for its strong structural properties, was taken as

Received: 13 May 2021 Revised: 18 July 2021
This work was supported by the National Natural Science Foundation of China (41877281).
First author: LIU Bing-heng, male, born in 1995, PhD candidate, research interests: mechanical properties of special soils. E-mail: liubingheng17@mails.ucas.ac.cn
Corresponding author: KONG Ling-wei, male, born in 1967, PhD, Research fellow, Doctoral supervisor, research interests: mechanical properties and disaster prevention technology of special soils. E-mail: lwkong@whrsm.ac.cn

the research object. Based on the previous researches in terms of its occurrence[16], stress path and strength characteristics under the influence of strain rate[17–18], true triaxial tests for various values of b and plane strain tests of undisturbed Zhanjiang structural clay were carried out by using the true triaxial test system, then the influence of structure on its mechanical properties and strength criterion was investigated under true three-dimensional stress state.

2 Soil sample and testing program

2.1 Soil sample

The soil samples were collected from a coastal site in Zhanjiang City, Guangdong Province, at a depth of 10–12 m. The less undisturbed samples were obtained by a thin wall sampler with a diameter of 20 cm, and its physical properties and particle composition are shown in Table 1. It can be seen that Zhanjiang clay could be described as soft clay owing to its properties of high water content, high void ratio, high clay composition and low permeability, but it had better mechanical properties than ordinary soft soil. The yield stress of undisturbed Zhanjiang clay was up to 350 kPa (Fig. 1), and the unconfined compressive strength was up to 110.6 kPa (Fig. 2), while the structure yield stress and unconfined compressive strength of Tianjin soft clay with a relatively weak structure at the same embedment depth were only 150 kPa and 57 kPa, respectively[19], which were far less than those of Zhanjiang clay.

Table 1 Basic physical properties and particle composition of Zhanjiang clay

Depth /m	Density ρ /(g·cm^{-3})	Specific gravity ρ_s /(g·cm^{-3})	Void ratio e	Water content w /%	Liquid limit w_L /%	Plasticity limit w_P /%	Plasticity index I_P	Permeability coefficient /(cm·s^{-1})	Particle composition /%	
									0.005–0.075 mm	<0.005 mm
10～12	1.71	2.73	1.45	53.11	62.2	28.8	33.4	2.7×10^{-8}	59.1	40.9

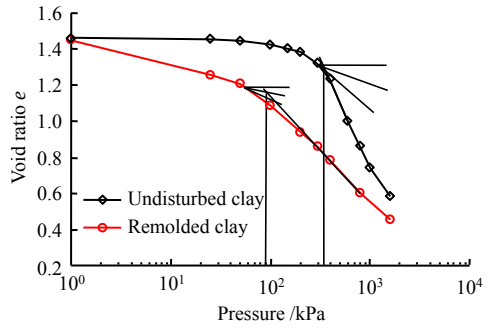

Fig. 1 Compression curves of undisturbed and remolded Zhanjiang clays

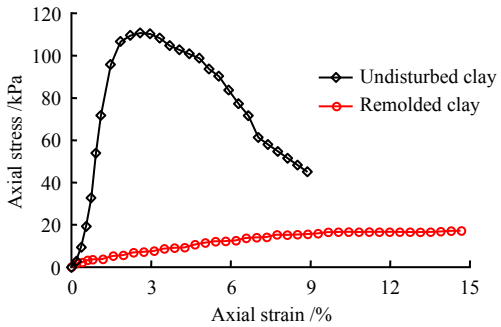

Fig. 2 Stress–strain curves of unconfined uniaxial compression tests on undisturbed and remolded Zhanjiang clays

Figure 1 demonstrates the compression curves of undisturbed clay and remolded clay. The pre-consolidation pressure P_c of undisturbed clay was up to 350 kPa, which was much greater than the overburden pressure. The compression curve of undisturbed clay differed markedly from the typical slow-falling compression curve of over-consolidated soil as it had an obvious yield point and steep descent stage, the high value of P_c of this soil should result from the performance of soil structured strength, but not originate from the over consolidation[20]. Therefore, the P_c of Zhanjiang clay should be regarded as the structure yield stress σ_k[16]. Fig. 2 shows the unconfined compression curves of undisturbed clay and remolded clay, the unconfined compressive strengths of the undisturbed clay and the remolded clay were 110.6 kPa and 17.2 kPa, respectively, the soil sensitivity S_t was greater than or equal to 6.4, which belonged to highly sensitive clay. Microscopic researches[16] illustrate that the structure of Zhanjiang clay mainly came from the metastable flocculated structure and intergranular cementation, and the soil was in an acidic environment with a pH of about 5.2 for a long time. The combination of the positively charged free iron oxide with the negatively charged clay colloids forms a strong bond between the particles, enhancing its structure.

2.2 Test instrument

The instrument used in the test was PX-2000 true triaxial instrument produced by GCTs company of the United States. The loading mode of the instrument was the rigid-flexible hybrid type. The major principal stress σ_1 and the intermediate principal stress σ_2 were applied by two pairs of rigid plates, respectively. The minor principal stress σ_3 was applied by the water pressure in the pressure chamber. Therefore, the instrument can independently control the values of σ_1, σ_2, σ_3 on the sample without interference to realize different loading paths of the sample in three-dimensional stress space.

2.3 Test scheme

A true triaxial apparatus was used to apply different loading paths to the specimens in three-dimensional stress space. The relationship between the three principal stresses was usually characterized by the intermediate principal stress ratio b:

$$b=\frac{\sigma_2-\sigma_3}{\sigma_1-\sigma_3} \quad (1)$$

At the beginning of the test, the undisturbed clay was taken out from the thin-walled sampler firstly,

then it was placed on the self-made true triaxial sample cutter and was cut into a cuboid of 160 mm × 75 mm × 75 mm in size by a wire saw. Because the large-size clay samples were difficult to be saturated, the cuboid samples were firstly saturated in the self-made cuboid saturator and then were saturated again by applying a back pressure of 200 kPa. When the saturation reached 0.98, the consolidation under different pressures was carried out. The consolidation process was completed as the pore water pressure dropped to 5% of the consolidation stress, and then the true triaxial tests (Table 2) were carried out.

Table 2 True triaxial tests and plane strain tests scheme

Test type	Mean principal stress p (consolidation stress) / kPa	Intermediate principal ratio b
True triaxial tests with different b values	100，200，300，400，600	0，0.25，0.5，0.75，1.0
Plain strain vertical loading test	200，400，600	—
Plain strain lateral unloading test	200，400，600	—

(1) In order to investigate the strength criterion in π plane, a series of true triaxial tests with b values were carried out. During tests, the mean principal stress p of the sample was kept as the consolidation pressure, and undrained shear tests of 0, 0.25, 0.50, 0.75 and 1.00 were performed. The total stress paths in π plane are shown in Fig. 3.

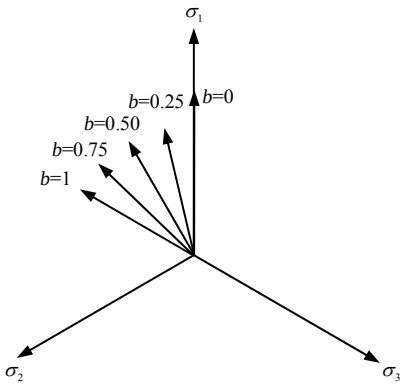

Fig. 3 Total stress path in π plane

(2) The soil in foundation pits or subgrades is often in the plane strain state. Therefore, the plane strain vertical loading and lateral unloading tests under different confining pressures were carried out: (a) the positions of the two plates in the control direction were unchanged to ensure the intermediate principal strain ε_2=0, and then the undrained shear tests of constant σ_3 and an increase of σ_1 were carried out; (b) The positions of the two plates in the control direction remained unchanged to ensure the intermediate principal strain ε_2=0, and then conduct the undrained shear test of constant σ_1 and reduced σ_3 were carried out.

3 Mechanical properties in three-dimensional stress state

3.1 Stress–strain relationships

Figure 4 illustrates the generalized shear stress q–principle strain ε_1 curves of Zhanjiang clay under p=100, 200, 300, 400, and 600 kPa and b = 1, 0.25, 0.50, 0.75, and 1.00, and plane strain loading and unloading conditions. As can be seen in Fig. 4, when p=100, 200, and 300 kPa, respectively, i.e., the consolidation stress was less than the structure yield stress σ_k=0350 kPa, the q–ε_1 curves exhibited strain-softening behavior. The strain-softening phenomenon occurred that q first rose to the peak and then decreased with the increase of ε_1, the peak of q was observed around 2%, except for the case of $b=1$. In contrast to the stress-strain relationships for other b values, there was no obvious strain-softening behavior in the q–ε_1 curves for $b=1$ and $p\leqslant 300$ kPa. Similar results can be found in the true triaxial test of Q_2 loess with 5% moisture content in the literature[21], for instance, when the consolidation stress was 50 kPa, the stress-strain curves showed obvious strain-softening behavior in the case of b=0, 0.25 and 0.50, while the stress-strain curves showed slight strain-hardening behavior under b=0.75 and 1.00. Reasons for the above experimental phenomena may be that the intermediate principal stress increased correspondingly with the increase of b, thus affecting the development of major principal strain during shearing and resulting in no significant decreasing trend after the increase of shear stress to the peak at b=1 and no significant strain-softening in the q–ε_1 curves. When p=400 and 600 kPa, i.e., the consolidation stress was greater than the structure yield stress σ_k, the q–ε_1 curves are of slight strain-hardening type, which had significant differences from that of soft clay with weak structure. In the literature[3−5], the stress–strain curves in the true triaxial test of soft clay under different confining pressures were strain hardening types, and there was no typical strain-softening phenomenon of structured clay under low confining pressure, indicating that the strong structure had a great impact on the stress–strain relationship of Zhanjiang clay. Dai et al.[22] found similar results in the true triaxial tests of Yingkou undisturbed soft clay. When the consolidation stress was less than or greater than the structure yield stress σ_k, the stress–strain relationship was the strain-softening or strain-hardening type, which reflected the effect of structure on the stress–strain relationship. When the consolidation stress was less than the structure yield stress, the structural damage of soil caused by the consolidation process was small, but the shear stress gradually increased in the shear process, and then decreased after reaching the peak, the soil structure failed and the strain-softening behavior appeared; when the consolidation stress was greater than the structure yield stress σ_k, the consolidation process caused great damage to the soil structure, making the stress–strain relationship similar to that of the clay with weak structure[23].

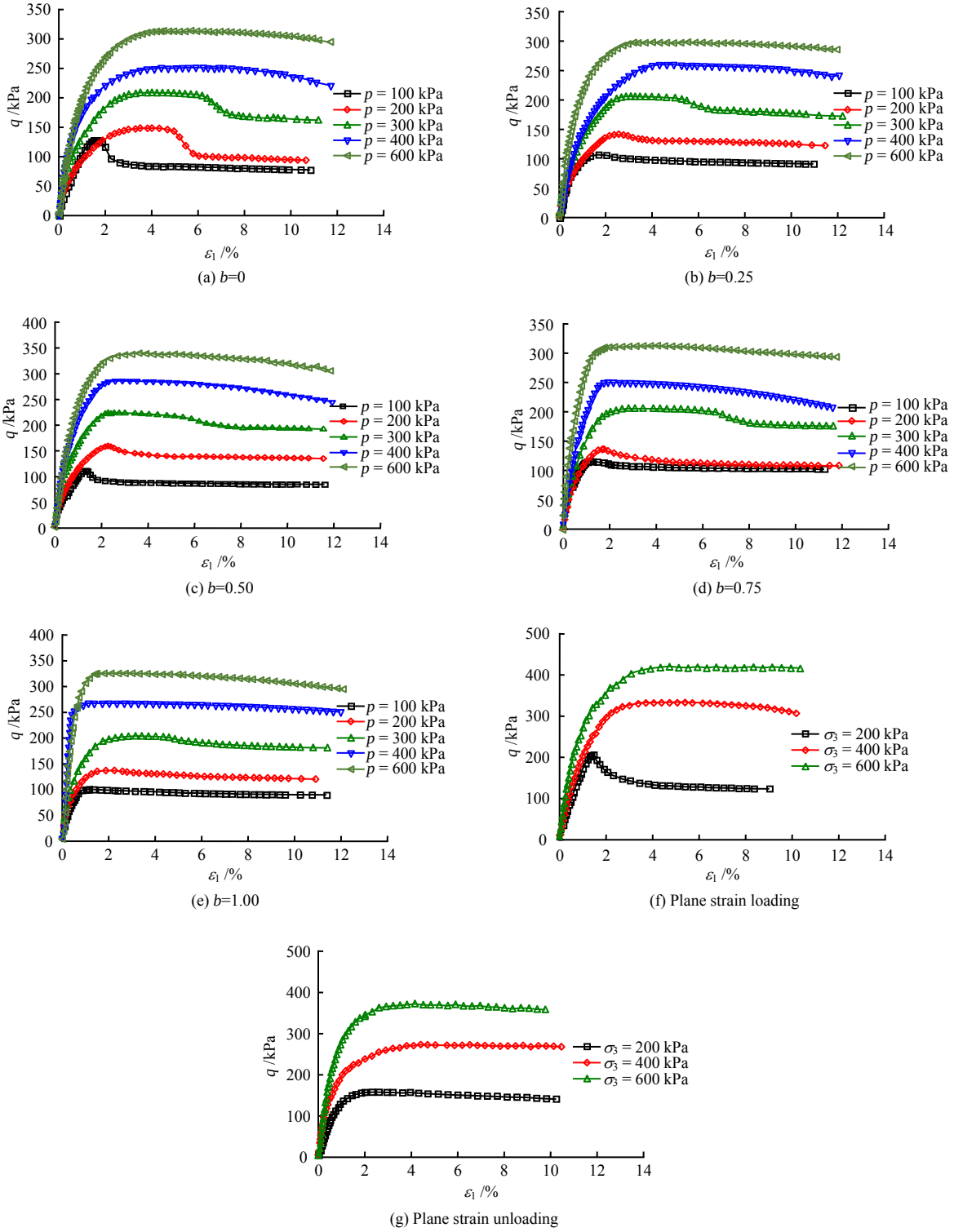

Fig. 4 Stress–strain curves of true triaxial tests with different *b*-values and plane strain compression tests

The q–ε_1 curves with the same p value and different b values are similar in behavior. As the b value increased, the major principal strain corresponding to the q peak point showed a decreasing trend. This might be due to the fact that the increase of intermediate principal stress limited the development of the major principal strain, thus shifting the peak value of q forward. The q–ε_1 curves under plane strain loading and unloading conditions were similar to those with different b values, and the major principal strain corresponding to the q peak point was close to those with $b = 0.25$ and 0.50. Fig. 5 presents the development of b from the beginning of shearing to the failure of the sample in the plane strain test. It can be seen from Fig. 5 that during the loading and unloading process of the plane strain test, the value of b first decreased and then increased with the major principal strain, and most of the b values were between 0.1 and 0.5. The above results showed that the stress paths of the plane strain loading and unloading test was close to that of the true

triaxial test in the cases of b=0.25 and 0.50, resulting in a similar stress–strain relationship between them.

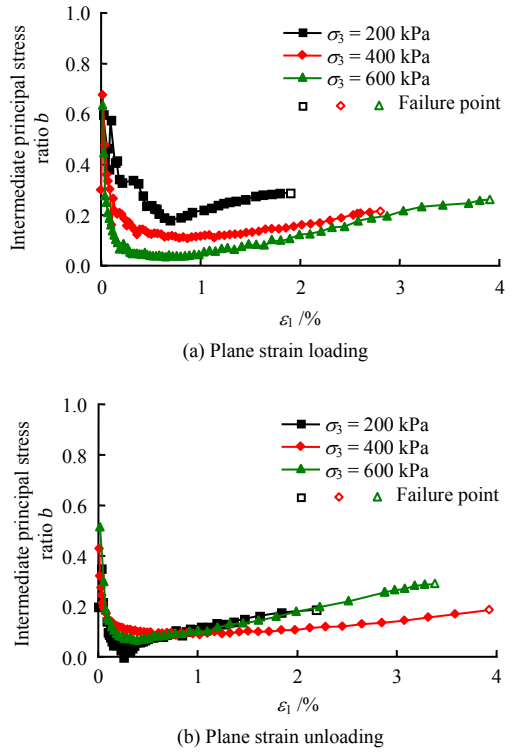

Fig. 5 Relationships between b-values and major principal strain before the failure of specimens in plane strain compression tests

3.2 Pore pressure–strain relationships

Figure 6 shows the pore water pressure u–ε_1 curves of Zhanjiang clay at p =100, 200, 300, 400, 600 kPa and b=0, 0.25, 0.50, 0.75, 1.00 in true triaxial texts and plane strain loading and unloading tests. It can be seen that the pore pressure–strain relationship was related to the consolidation stress. The overall pore pressure showd a behavior of increasing to peak and then decreasing with the strain development. Comparing the triaxial test results of two clays with different structural properties (Shanghai clay and Zhanjiang clay) in the literature[24], the pore pressure–strain curves of the weaker structural clay showed a peak in the case of low consolidation pressure, in other case the pore pressure-strain curves were monotonically increased. When the consolidation stress of strong structured clay was less than the structure yield stress σ_k, the pore water pressure decreased rapidly after the obvious peak value. While the pore pressure decreased slowly after the peak as the consolidation stress was greater than the structure yield stress. The development of pore pressure at p = 600 kPa was different from those with different p values, and its pore pressure peak was significantly greater than those under other conditions. On the one hand, the peak pore pressure was in accordance with the general rule that it increased with the increase consolidation stress. On the other hand, the soil structural damage was small when the consolidation stress was less than the structure yield stress, the load on the strong structured clay was mainly borne by soil skeleton, and the pore pressure was restrained by the strong inter-particle cementation; when the consolidation stress was siginificantly higher than the structure yield stress σ_k, the soil structure was greatly damaged, the void ratio and permeability coefficient reduced sharply, and the inter-particle cementation between was weakened, resulting in a great increase in the pore pressure peak when the soil was subjected to the external loads[23]. In addition, the major principal strain corresponding to the peak pore pressure was slightly greater than that corresponding to the peak value q, that is, there was a slight pore pressure lag in the undrained shear process of Zhanjiang clay. In the plane strain unloading test, with the increase of the major principal strain, the pore water pressure was always negative and decreased monotonically, indicating that the soil was always in dilatancy state during the unloading process.

3.3 Effect of b on internal friction angle and cohesion force

Mohr circles are plotted in Fig. 7 based on the stress values at the failure point of true triaxial tests and plane strain tests with different b values, where σ and τ are the normal stress and shear stress, respectively. Then the effective strength indexes of true triaxial tests and plane strain tests with different b values were obtained. Fig. 8 illustrates the relationship between the effective cohesion force c', the effective internal friction angle φ' and the b value. The values of c' and φ' were not equal for different b values but varied with b values. On the whole, c' decreased with the increase of b, and c' was equal to 36.98 kPa and 20.95 kPa, respectively, in the case of b=0 and 1, which was reduced by 43.3%. φ' increased with the increase of b, and φ' was equal to 14.83° and 22.74° respectively, in the case of b=0 and 1, which was increased by 53.3%. The superimposed effect of intermediate principal stress on the soil compaction and structural damage might be responsible for the variation of effective cohesion and friction angle. The intermediate principal stress increased with b, resulting in further soil compaction and an increase of friction angle. At the same time, the damage of soil structure and the decrease of cohesion were also induced.

From the plane strain test results in Fig. 7, the corresponding c' and φ' in the plane strain test with loading and unloading were 37.25 kPa, 19.27° and 38.53 kPa, 18.51°, respectively, with values between those of true triaxial tests with b=0.25 and 0.50. The reason was that most of the b values were between 0.1–0.5 before sample failure and 0.18–0.29 at the failure point.

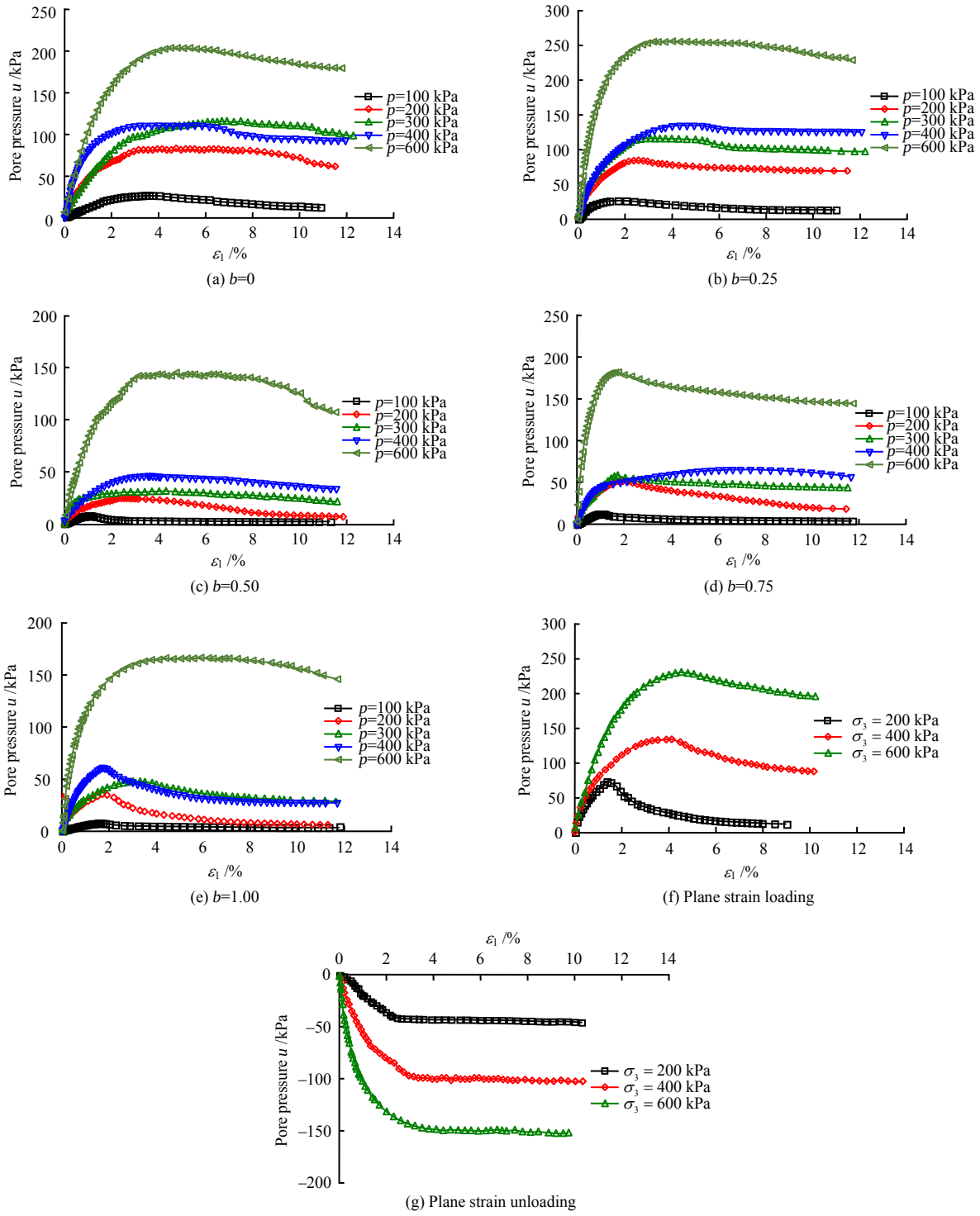

Fig. 6 Pore pressure–strain curves of true triaxial tests with different *b* values and plane strain compression tests

4 Strength criterion

4.1 Strength criterion in π plane

After analyzing the strength data of the above failure points, it was found that the effective mean principal stress p' had a linear relationship with q in the meridian plane at soil sample failure under the same intermediate principal stress ratio b. It was more appropriate to fit by the formula ($q = Ap' + B$) (Fig. 9), where A and B are the slope and intercept of the fitted curve, respectively. The strength criterion commonly used in engineering are

Mises criterion:

$$\sqrt{J_2} = k_{\mathrm{m}} \tag{2}$$

where J_2 is the second invariant of deviatoric stress tensor; and k_{m} is the material constant.

Mohr-Coulomb criterion:

$$\frac{I_1}{3}\sin\varphi - \sqrt{J_2}\left(\frac{1}{\sqrt{3}}\sin\theta\sin\varphi + \cos\theta\right) + c\cos\varphi = 0 \tag{3}$$

where I_1 is the first invariant of effective stress tensor; θ is the stress lode angle; c is the cohesion; and φ is the internal friction angle.

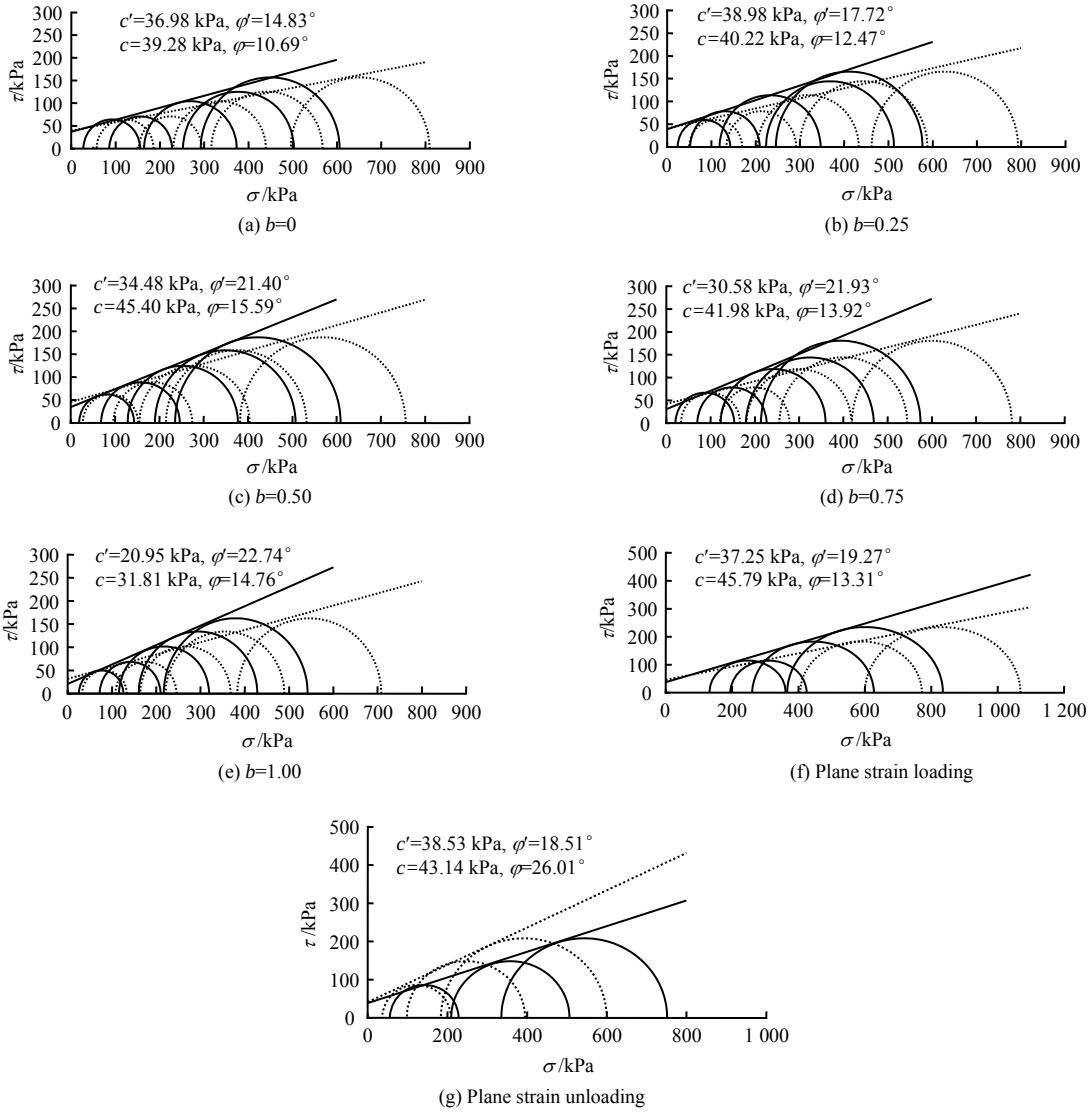

Fig. 7 Mohr envelopes of true triaxial tests with different *b* values and plane strain compression tests

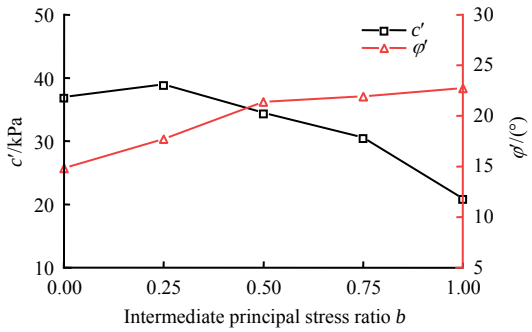

Fig. 8 Influence of intermediate principal stress ratio on effective cohesion and internal friction angle

Lade-Duncan criterion:

$$\frac{I_1^3}{I_3} = k_f \tag{4}$$

where I_3 is the third invariant of effective stress tensor; and k_f is the material constant.

The effective mean principal stress with different *p* values at *b*=0 was taken as the effective mean principal stress of failure points with varying values of *b* at different consolidation stress levels. According to Fig. 8 and Fig. 9, the strength data of failure points at 100, 200, 300, 400, and 600 kPa were obtained respectively to reflect the shape of failure envelopes of Zhanjiang clay under the test conditions of this paper, and the calculated results of the strength criterion based on Eqs. (2) to (4) were plotted in π plane, as shown in Fig. 10.

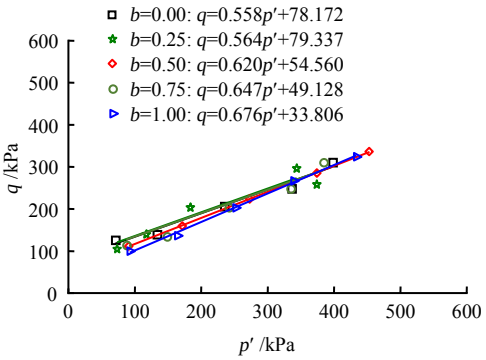

Fig. 9 Failure envelopes in the *p′*–*q* plane

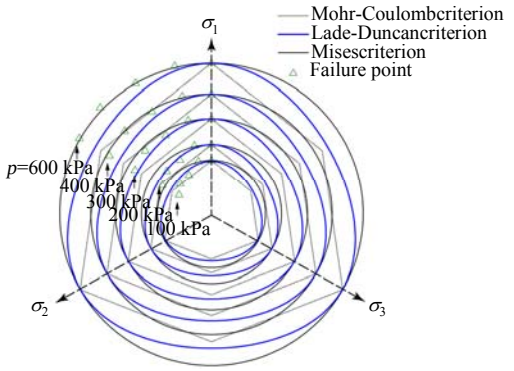

Fig. 10 Failure loci in π plane

As can be seen from Fig. 10, the Mohr-Coulomb criterion underestimated the strength of failure point in π plane under all p value conditions, because the contribution of the intermediate principal stress to the strength was not considered; the Lade-Duncan criterion agreed well with the failure point at p=100, 200 and 300 kPa, while it underestimated the failure point at p=400 and 600 kPa. The phenomenon of outward deviation of the failure point was similar to the experimental results in the literature[25–26]. The failure point of Zhanjiang clay under three-dimensional stress state at p=400 and 600 kPa was between the Mises criterion and the Lade-Duncan criterion. For this reason, according to the literature[27], the generalized nonlinear strength theory based on the Mises criterion and the Lade-Duncan criterion was introduced to describe the failure point strength of Zhanjiang clay at $p \geqslant 400$ kPa. The generalized nonlinear strength theory was expressed by the shear stress q_c and invariants of principal stress at failure in the case of $b = 0$:

$$q_c = \alpha q_M + (1-\alpha) q_L \tag{5}$$

where α is the tension–compression ratio in π plane; q_M is the shear stress corresponding to the Mises criterion; and q_L is the shear stress corresponding to the Lade-Duncan criterion.

$$q_M = \sqrt{I_1^2 - 3I_2} \tag{6}$$

$$q_L = I_1 \left\{ 1 - \frac{1}{2}\sqrt{\frac{27I_3}{I_1^3}} \left[\cos\left(\frac{1}{3}\cos^{-1}\left(-\sqrt{\frac{27I_3}{I_1^3}} \right) \right) \right]^{-1} \right\} \tag{7}$$

where I_1, I_2, and I_3 are the invariants of the effective stress tensor. When $\alpha = 1$, this criterion can be simplified as the Mises criterion; when $\alpha = 0$, this criterion can be simplified as the Lade-Duncan criterion.

From the calculation, the generalized nonlinear strength criterion in the case of $\alpha = 0.85$ was consistent with the failure point strength at 400 and 600 kPa, that is, it was more reasonable to choose the generalized nonlinear strength criterion when p was greater than 400 kPa. Fig. 11 shows the comparison between the strength criterion and the failure point strength at 100, 200, 300, 400 and 600 kPa. Combined with the failure loci in Fig. 10, it was found that the failure point strength was close to the Lade-Duncan criterion when p was less than 300 kPa; and it deviated gradually from the locus of Lade-Duncan criterion in π plane with the increase of p, the shape of envelopes gradually tended to circle, and it was more appropriate to adopt the generalized nonlinear strength criterion based on the Mises and Lade-Duncan criteria. Similar results can be found in the literature[25–26] for investigating the strength criterion of Q_2 and Q_3 loess. Failure loci expanded with the increase of effective mean principal stress, and the shape of failure loci also changed. However, the variation of failure loci shape in this paper was not consistent with those in the literature[25–26], the change of the failure point and failure loci were more pronounced, indicating that there was an apparent mutation in the strength criterion of strong structured Zhanjiang clay before and after yield.

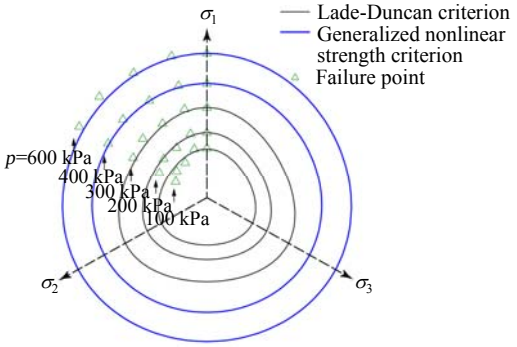

Fig. 11 Strength criterion in π plane

The failure loci shapes of Zhanjiang clay in π plane changed significantly before and after $p = 400$ kPa. The reason is that its strength was not only affected by the intermediate principal stress, but also its structure. In the literature[28], the microstructure changes of the in-situ Zhanjiang clay after different consolidation pressures were obtained based on scanning electron microscopy. It was found that the in-situ Zhanjiang clay was an open flocculated structure, with the basic units showing a hollow form, no directional arrangement, less point contact and high porosity development. When the consolidation pressure was less than σ_k, the contact mode between the pore volume and the particle did not change significantly, and its structure damage was minor; when the consolidation pressure was greater than σ_k, the pore volume decreased obviously, the inter-particles contact mode was gradually transformed into the face-to-face mode where the particle arrangement tended to be ordered, and the hollow structure was progressively transformed into the lamellar structure, which was close to the microstructure of remolded soil, and its structure was almost lost. The microstructure of Zhanjiang clay changed greatly before or after the structure yield stress σ_k. Based on the general law that the macro mechanical properties of soil are controlled by the microstructure, the shape of failure loci changes before and after the consolidation pressure is σ_k.

4.2 Strength criterion under plane strain condition

Based on the fact that the soil is in plane strain state in many cases, there are some differences in stress path and sample boundary conditions between plane strain test and true triaxial test with different b values[29]. It is worth exploring whether the strength criterion of Zhanjiang clay in the true triaxial test is applicable to its plane strain condition.

From Fig. 5, under the shear process of Zhanjiang clay in plane strain tests, most of the b values were in the range of 0.1–0.5 before the soil reached the peak point. The value of b was between 0.20–0.29 in vertical loading tests, and 0.18–0.29 in lateral unloading tests. Fig. 11 shows that it was more appropriate to use the Lade-Duncan criterion or generalized nonlinear criterion to describe the failure point when the consolidation stress was lower or greater than σ_k. According to the consolidation stress, the two above strength criteria were used to describe the failure point under plane strain conditions, as shown in Fig. 12. Overall, the strength criterion of Zhanjiang clay under the true triaxial test was basically suitable for the plane strain condition. Because the value of b in the plane strain test changed continuously in an interval, rather than keeping constant at failure, there would be some errors when using the strength criterion under the true triaxial condition.

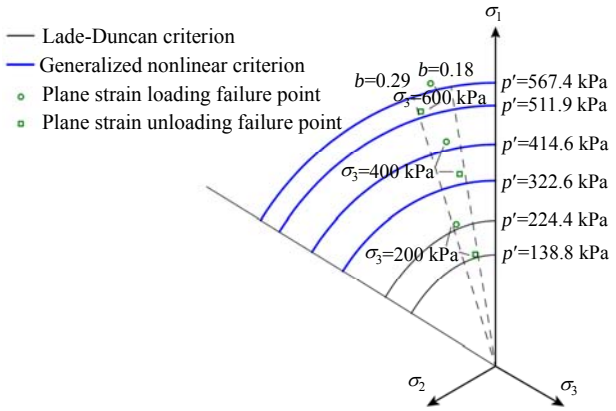

Fig. 12 Strength criterion under plane strain condition

In order to better describe the strength criterion of Zhanjiang clay under plane strain conditions, the plane strain test results of Zhanjiang clay were analyzed by using generalized Mises plane strain strength criterion and Lade-Duncan plane strain strength criterion[30].

Generalized Mises plane strain strength criterion:

$$\sigma_1 = K_{\text{P-MIS}}\sigma_3 + c'\cot\varphi'(K_{\text{P-MIS}} - 1) \tag{8}$$

where $K_{\text{P-MIS}} = \dfrac{1 + K_{\text{MIS}} + \sqrt{6K_{\text{MIS}} - 3K_{\text{MIS}}^2}}{1 - 2K_{\text{MIS}}}$, $K_{\text{MIS}} = \dfrac{2(K_{\text{P}} - 1)^2}{(K_{\text{P}} + 2)^2}$, $K_{\text{P}} = \tan^2(45° + \varphi'/2)$.

Lade-Duncan plane strain strength criterion:

$$\sigma_1 = K_{\text{P-LD}}\sigma_3 + c'\cot\varphi'(K_{\text{P-LD}} - 1) \tag{9}$$

where $K_{\text{P-LD}} = \dfrac{2}{27}K_{\text{LD}} + \dfrac{2}{27}\sqrt{K_{\text{LD}}^2 - 27K_{\text{LD}}} - 1$, $K_{\text{LD}} = \dfrac{(K_{\text{P}} + 2)^3}{K_{\text{P}}}$.

In the two above plane strain strength criteria, the intermediate principal stress at failure point can be obtained by the following equation.

The intermediate stress of generalized Mises plane strain strength criterion at failure:

$$\sigma_2 = \frac{\sigma_1^2 + \sigma_3^2}{\sigma_1 + \sigma_3} \tag{10}$$

The intermediate stress of Lade-Duncan plane strain strength criterion at failure:

$$\sigma_2 = \frac{\sigma_1 + \sigma_3}{2} \tag{11}$$

The test results under plane strain conditions are analyzed according to Eqs. (8), (10) and Eqs. (9) and (11), the effective strength of Zhanjiang clay under plane strain loading and unloading conditions and the calculated failure loci of generalized Mises and Lade-Duncan plane strain strength criteria are plotted together in drawn in Fig. 13 in the p'–generalized shear stress q coordinate, the expressions of p'–q failure loci of generalized Mises and Lade-Duncan plane strain strength criteria were obtained in Fig. 13. The strength of generalized Mises plane strain strength criterion is greater than that of Lade-Duncan plane strain strength criterion. The strength of Zhanjiang clay plane strain test was between the generalized Mises and Lade-Duncan plane strain strength criteria, which was similar to the results of true triaxial test in section 4.1. Therefore, a generalized plane strain strength criterion based on generalized Mises and Lade Duncan plane strain strength criteria was proposed to describe the plane strain test results of Zhanjiang clay. In a certain p' condition, the plane strain strength q of Zhanjiang clay was the combination of the two above strength criteria:

$$q = \beta q_{\text{MIS}} + (1 - \beta)q_{\text{LD}} \tag{12}$$

where q_{MIS} and q_{LD} are the q of generalized Mises and Lade-Duncan plane strain strength criteria under the same effective mean principal stress p' condition.

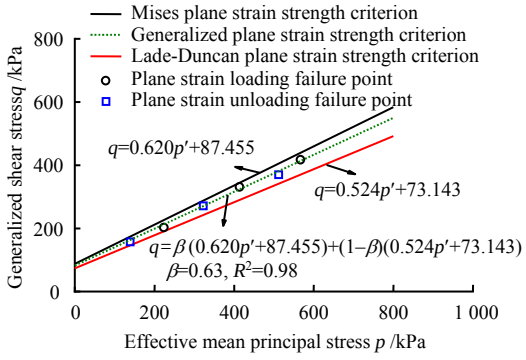

Fig. 13 Strength criterion under plane strain condition in p'–q plot

The test results are fitted by Eq. 12, both the obtained failure loci and the test results are drawn in Fig. 13. It can be found that the proposed generalized plane strain strength criterion can better describe the strength of Zhanjiang clay in plane strain test.

5 Conclusions

(1) Due to the influence of structure, when p was less than or greater than the structure yield stress σ_k, the $q-\varepsilon_1$ curve of Zhanjiang clay was of strain softening and mild strain hardening type, respectively. The $q-\varepsilon_1$ curves of true triaxial tests with different b values had similar patterns, but the major principal strain corresponding to the q peak decreased with the increase of b value.

(2) Overall, the effective cohesion decreased with the increase of b value, while the effective internal friction angle increased. In the plane strain test, the b value remained in the range of 0.1–0.5 before failure, then the values of effective cohesion and friction angle were between those corresponding to $b=0.25$ and $b=0.5$.

(3) The strength criterion of Zhanjiang clay under the true three-dimensional stress state was affected by structure, and the failure envelope changed around $p=400$ kPa. The strength criterion of Zhanjiang clay in π plane agreed well with the Lade-Duncan criterion when p was less than the structure yield stress. And beyond that, satisfactory results were obtained with generalized nonlinear strength criterion based on Mises and Lade-Duncan criteria.

(4) In the plane strain test, the b value of Zhanjiang clay at failure was in the range of 0.18–0.29. The failure strength can be approximately described by the generalized plane strain strength criterion based on the generalized Mises and Lade-Duncan plane strain strength criteria, which provided a new way to establish the strength criterion of structured clay under plane strain conditions.

References

[1] ZHANG Min, XU Cheng-shun, DU Xiu-li, et al. True triaxial experimental research on shear behaviors of sand under different intermediate principal stresses and different stress paths[J]. Journal of Hydraulic Engineering, 2015, 46(9): 1072–1079.

[2] WOOD D M. Explorations of principal stress space with kaolin in a true triaxial apparatus[J]. Géotechnique, 1975, 25(4): 783–789.

[3] CALLISTO L, CALABRESI G. Mechanical behaviour of a natural soft clay[J]. Géotechnique, 1998, 48(4): 495–513.

[4] SUN H, WANG H L, WU G, et al. The mechanical properties of naturally deposited soft soil under true three-dimensional stress states[J]. Geotechnical Testing Journal, 2019, 42(5): 1370–1383.

[5] SUN Hong, YUAN Ju-yun, ZHAO Xi-hong. Study on soft soil by the true triaxial tests[J]. Journal of Hydraulic Engineering, 2002, 33(12): 74–78.

[6] PRASHANT A, PENUMADU D. A laboratory study of normally consolidated kaolin clay[J]. Canadian Geotechnical Journal, 2005, 42(1): 27–37.

[7] KIRKGARD M M, LADE P V. Anisotrotropy of normally consolidated San Francisco Bay mud[J]. Canadian Geotechnical Journal, 1991, 14(3): 231–246.

[8] ANANTANASAKUL P, YAMAMURO J A, LADE P V. Three-dimensional drained behavior of normally consolidated anisotropic kaolin clay[J]. Soils and Foundations, 2012, 52(1): 146–159.

[9] LADE P V. Elasto-plastic stress-strain theory for cohesionless soil with curved yield surfaces[J]. International Journal of Solids Structures,1977, 13(11): 1019–1035.

[10] MATSUOKA H, NAKAI T. Stress-deformation and strength characteristics of soil under three different principal stresses[C]//Proceedings of the Japanese Society of Civil Engineers. [S. l]: [s. n.], 1974: 59–70.

[11] YU Mao-hong. New system of strengh theory[M]. Xi′an: Xi′an Jiaotong University Press, 1992.

[12] GONG Xiao-nan, XIONG Chuan-xiang, XIANG Ke-xiang, et al. The formation of clay structure and its influence on mechanical characteristics of clay[J]. Journal of Hydraulic Engineering, 2000, 31(10): 43–47.

[13] WANG Li-zhong, LI Ling-ling. Field disturbance of structured clay and its effect on settlements of soil foundation[J]. Chinese Journal of Geotechnical Engineering, 2007, 29(5): 697–704.

[14] JIA Rui, LEI Hua-yang. Experimental study of anisotropic consolidation behavior of Ariake clay[J]. Rock and Soil Mechanics, 2019, 40(6): 2231–2238.

[15] BURLAND J B, RAMPELLO S, GEORGIANNOU V N, et al. A laboratory study of the strength of four stiff clays[J]. Géotechnique, 1996, 46(3): 491–514.

[16] TUO Yong-fei, KONG Ling-wei, GUO Ai-guo, et al. Occurrence and engineering properties of structural soft clay in Zhanjiang area[J]. Rock and Soil Mechanics, 2004, 25(12): 1879–1884.

[17] KONG Ling-wei, ZANG Meng, GUO Ai-guo, et al. Effect of stress path on strength properties of Zhanjiang strong structured clay[J]. Rock and Soil Mechanics, 2015, 36(Suppl.1): 19–24.

[18] CAI Yu, KONG Ling-wei, GUO Ai-guo, et al. Effects of shear strain rate on mechanical behavior of Zhanjiang strong structured clay[J]. Rock and Soil Mechanics, 2006,

27(8): 1235−1240.

[19] XIONG Chun-fa. Characteristic of mechanics reponse and structural damage of soft clay under different loading mode[D]. Wuhan: Institute of Rock and Soil Mechanics, Chinese Academy of Sciences, 2016.

[20] SHEN Zhu-jiang. Engineering properties of soft soils and design of soft ground[J]. Chinese Journal of Geotechnical Engineering, 1998, 21(1): 100−111.

[21] ZHANG Jian-hui. Research on the strengh, deforamtion and damage characteristics of Q_2 loess based on true triaxial tests[D]. Xi'an: Xi'an University of Technology, 2009.

[22] DAI Jin-qiu, SU Zhong-jie, ZHAO Ming-chao, et al. True triaxial tests on stress-strain characteristics of soft clay considering the structural effects[J]. Chinese Journal of Rock Mechanics and Engineering, 2017, 36(4): 997−1004.

[23] CAI Yu. Research on time-dependent mechanical behavior of strong structured clay in Zhanjiang area[D]. Wuhan: Institute of Rock and Soil Mechanics, Chinese Academy of Sciences, 2005.

[24] ZHANG Cheng-hou. Geotechnical characteristics of two structure clays[J]. Hydro-Science and Engineering, 1983(4): 65−71.

[25] YU Qing-gao, SHAO Sheng-jun, SHE Fang-tao, et al. Research on failure modes and strength characteristics of Q_2 loess under true triaxial condition[J]. Rock and Soil Mechanics, 2010, 31(1): 66−70.

[26] SHAO S, SHAO S J, XU P. Anisotropic strength characteristics of loess under three-dimensional stress conditions[J]. Journal of Testing and Evaluation, 2019, 47(4): 2435−2450.

[27] YAO Yang-ping, LU De-chun, ZHOU An-nan, et al. Generalized nonlinear strength theory and transformed stress space[J]. Scientia Sinica (Series E), 2004, 34(11): 1283−1299.

[28] ZANG Meng. Research on structual damage of engineering behavior and dynamic characteristics for Zhanjiang structured clay[D]. Wuhan: Institute of Rock and Soil Mechanics, Chinese Academy of Sciences, 2016.

[29] JIANG Jing-shan, ZUO Yong-zhen, CHENG Zhan-lin, et al. Effects of stress state on mechanical properties of coarse granular material using large-scale true triaxial tests[J]. Rock and Soil Mechanics, 2020, 41(11): 3563−3572.

[30] ZHANG Yu, SHAO Sheng-jun, WANG Li-qin, et al. Analysis and verification of soil strength criteria in plane strain state[J]. Rock and Soil Mechanics, 2015, 36(9): 2501−2509.